ZIBELINE INTERNATIONAL™ PUBLISHING

ISSN: 2521-0920 (Print)
ISSN: 2521-0602 (Online)
CODEN: MJGAAN

Malaysian Journal of Geosciences (MJG)

DOI: http://doi.org/10.26480/mjg.02.2023.173.179

CrossMark

RESEARCH ARTICLE

ESTIMATION OF SHALLOW WATER BATHYMETRY ALONG THE NORTHERN COAST OF BAY OF BENGAL: A REMOTE SENSING-BASED APPROACH

Md. Abid Hasan[a], Rafid Fayyaz[b], Mahfujur Rahman[c], Mahmudul Hasan[b*], Md. Atikul Islam[b], Shamiha Shafinaz Shreya[b]

[a]Department of Oceanography, Noakhali Science and Technology University, Noakhali-3814, Bangladesh
[b]Department of Oceanography, University of Dhaka, Dhaka-1000, Bangladesh
cDepartment of Geology, University of Dhaka, Dhaka-1000, Bangladesh
[*]Corresponding Author Email: mahmud.hasan@du.ac.bd

ARTICLE DETAILS

Article History:

Received 20 November 2023
Revised 24 December 2023
Accepted 28 January 2024
Available online 03 February 2024

ABSTRACT

Bathymetric information is vital for navigational safety and is utilized for many more activities. Remote sensing data and satellite images are widely used these days to determine shallow coastal areas' bathymetry at a low cost. This study reviewed different methods for satellite-derived bathymetry and selected the ratio transform method to apply to Landsat 8 imagery. Two images covered the northern coastal region of the Bay of Bengal. They were processed using a ratio-based algorithm calibrated with reference data. A hydrographic chart from the Bangladesh Navy depicted a general overview of the study area. Another chart from the BIWTA, along with GEBCO gridded bathymetry data, was used as reference data for the study. The ArcGIS and ENVI image processing software was used to process and analyze satellite imagery. The correlation between the satellite-derived bathymetry and reference data was also studied at the end of the study. The mean absolute deviation, mean squared error, and root mean square error were also evaluated. Both algorithms were able to extract bathymetry up to a depth of 12 meters with minimal errors. Satellite Derived Bathymetry (SDB) from the Central Coast resulted in an R-squared value of 0.82 with a Mean Absolute Deviation (MAD) of 0.89. SDB from the Western Coast had R^2 of 0.81 and MAD of 1.16. After interpolating the algorithm results, contour lines were also generated to visualize the bathymetry. The deviations and irregularities in the contours resulted due to the high turbidity of the coastal waters of the Bay of Bengal.

KEYWORDS

Satellite-derived bathymetry; Ratio transform algorithm; Remote sensing; Bay of Bengal

1. INTRODUCTION

Bathymetric information, generally the data about water depth and submerged topography of lakes and oceans, is essential in numerous parts of marine and lacustrine exploration, organization, spatial configuration, and their assets (Hell et al., 2012). In any analysis of coastal processes such as – estuarine circulation, delta morphology, sediment transport, and reef ecology, accurate bathymetry is an essential first step (Geyman & Maloof, 2019). There is an apparent need for water depth measurements, especially in shallow areas that can pose a risk to navigation. Due to erosion and deposition, these areas are subject to rapid changes, particularly during storms (Lyzenga et al., 2006). Bathymetry assessment of oceans is an essential parameter that plays a notable role in modeling nearshore construction activities, such as managing ports, engineering work, laying pipelines, oil drilling, dredging activity, fishing, and aquaculture. Determining underwater topography, sediment movement and generating hydrographic charts for safe navigation is also very important, which depends on bathymetry estimation (Pushparaj & Hegde, 2017). Water depths were obtained using traditional techniques such as marked ropes or lead lines attached to the vessel that was released to hit the seafloor. This approach can be used to determine the depth of specific points in time; however, it is inefficient regarding the case of time and effort (Jagalingam et al., 2015).

To address this shortcoming, this approach was soon overtaken by the echo-sounding methods that use acoustic waves. Significant proportions of data that we receive from aquatic environments are now conveyed by sound waves, similar to how electromagnetic waves carry information above water (Lurton, 2002). The single and multi-beam are the two types of echo sounders that possess a transducer and a receiver. Multi-beams are preferred over single-beam echo sounders as they can transmit signals at a broader range, and acoustic waves are garnered from numerous points (Jagalingam et al., 2015; Lurton, 2002). Crucial drawbacks to acoustic measurements are the time and expenditure associated with field measurements. In this method, several survey lines with overlapping trails must be directed to assemble uniform bathymetry data. And that is why other approaches are being pursued to facilitate the pace of water depth acquisition (Elhassan, 2015).

Light Detection and Ranging (LiDAR) and Synthetic Aperture Radar (SAR) are also used in bathymetry estimation. LiDAR uses a stack of two waves (generally a mix of visible and infrared), one that penetrates the water column well and the other that bounces off the surface (Ma et al., 2020). The bathymetry is extracted by comparing the difference between those two incoming waves. SAR technique, on the other hand, uses long-wave electromagnetic radiation or radio waves to determine water depth. While LiDAR can provide precise estimations, it is constrained by its costly purchasing and servicing expenses(Leder et al., 2020). Unmanned Vehicle Systems like Autonomous Surface Vehicles, Autonomous submarine vehicles, and Remotely Operated submarine-vehicle that are utilized for

Quick Response Code	Access this article online	
	Website: www.myjgeosc.com	**DOI:** 10.26480/mjg.02.2023.173.179

Cite the Article: Md. Abid Hasan, Rafid Fayyaz, Mahfujur Rahman, Mahmudul Hasan, Md. Atikul Islam, Shamiha Shafinaz Shreya (2023). Estimation of Shallow Water Bathymetry Along the Northern Coast of Bay of Bengal: A Remote Sensing-Based Approach. *Malaysian Journal of Geosciences, 7(2): 173-179.*

various purposes can also be used in bathymetry estimation. However, their purchasing and maintenance expenses also limit these convenient devices (Leder et al., 2020; Romano & Duranti, 2012).

Most of the approaches outlined above need a significant interval between visits to a certain location, making it hard to detect changes in bathymetry. Shallow water bathymetry is essential for numerous pursuits, but these regions are challenging to be navigated with hydrographic vessels (Ma et al., 2014). The remote sensing approach that uses remotely sensed data with in-situ measurements is nowadays considered a promising substitute for calculating shallow water bathymetry (Winterbottom & Gilvear, 1997). Remote sensing technology can cover a larger region with repeated visits to the exact location over a short interval, and the data is conveniently accessible. In areas where coastal environments change rapidly, this method offers an efficient way to measure the bathymetry and detect even minor changes (Deng et al., 2008). The basic physical concept that water absorbs or attenuates light is the foundation of all algorithms for water depth extraction using satellite imagery. Both empirical and analytical algorithms are used in bathymetry estimation and data extraction from satellite imagery. The analytical approaches require multiple parameters dependent on the seafloor, water layer, and atmospheric constituents, making these challenging to be executed. Empirical techniques, on the other hand, demand fewer parameters making these less complicated while implementing (Adler-Golden et al., 2005; Geyman & Maloof, 2019; Kerr et al., 2018 Lyzenga, 1981). Relying upon the Beer-Lambert Law that establishes a log-linear interaction between electromagnetic reflectance and water depth, Lyzenga (1978, 1981) developed a simple algorithm to determine bathymetry from remotely sensed data. The algorithm has extensively been adjusted and employed for bathymetry estimation in shallow coastal territories as it is plain and efficacious (Dierssen et al., 2003; Figueiredo et al., 2016; Hogrefe et al., 2008; Liang et al., 2017; Lyzenga et al., 2006; Misra et al., 2018).

Lyzenga's linear approach has the flaw of assuming a consistent seabed reflectance. Therefore, estimations of bathymetry for specific bottom habitats might be misleading. Using a band ratio of two different spectral reflectances can be used to assess depth irrespective of bottom characteristics (Kanno et al., 2012). Reflectance ratios between separate bands are less susceptible to bottom albedo since the attenuation of light underwater can vary depending on different wavelengths. This ratio algorithm, however, couldn't perform efficiently in locations with significantly varying bottom types, leading several authors to adopt more advanced methods like machine learning approaches and artificial neural networks. These approaches are unique compared to all other techniques for deriving bathymetry. They require no direct use of water optical parameters such as attenuation, reflectance, or other physical properties to process the image for extracting bathymetry. However, training the technique requires a great deal of in-situ depth data that can restrict its utility. Support Vector Machines, for example, can be used to predict bathymetry accurately, but several studies attempted to extrapolate water depths outside the calibration data, and they came up with inaccurate estimates (Ceyhun & Yalçın, 2010; Doxani et al., 2012; Eugenio et al., 6357; Gholamalifard et al., 2013; Liu et al., 2015; Lyons et al., 2011; Makboul et al., 2017; Stumpf et al., 2003).

Geyman and Maloof (2019) introduced a Cluster-Based Regression or CBR algorithm that initially segments the satellite image into regions of spectral similarity. Then the log-linear color-to-depth relationship is calibrated individually for each cluster. This approach extends the Stumpf et al. (2003) ratio approach by utilizing several band ratios to extract additional knowledge from remotely sensed imagery. In addition to reducing bias and error, the CBR approach measures depth variability and provides better bathymetry estimations over varying bottom types (Geyman & Maloof, 2019). The band ratio approach is advantageous for this study as it tends to be reasonably easy to implement and can be tuned with water depth information at two or more stations. The CBR and band ratio algorithm perform satisfactorily while extrapolating outside the calibration dataset, and each can be implemented on multispectral satellite imagery. So, we decided to employ the band ratio method or the Ratio Transform Algorithm of Stumpf et al. (2003) with the concept of Cluster-Based Regression developed by (Geyman & Maloof, 2019).

2. Study Area

The study area encompassed almost the entire coast of Bangladesh, stretching from the Sundarbans mangrove forest in the west to Cox's Bazar in the east. The Landsat image with WRS Path 137 and Row 45 encompasses the western and a portion of the central coast of Bangladesh, including Sundarbans, the world's largest mangrove forest. On the other hand, the image with Path 136 and Row 45 mostly covers the central part and a segment of the eastern coast. The study area is dynamic, with phenomena originating from extreme sediment input, human intervention, and infrastructural developments on the shore.

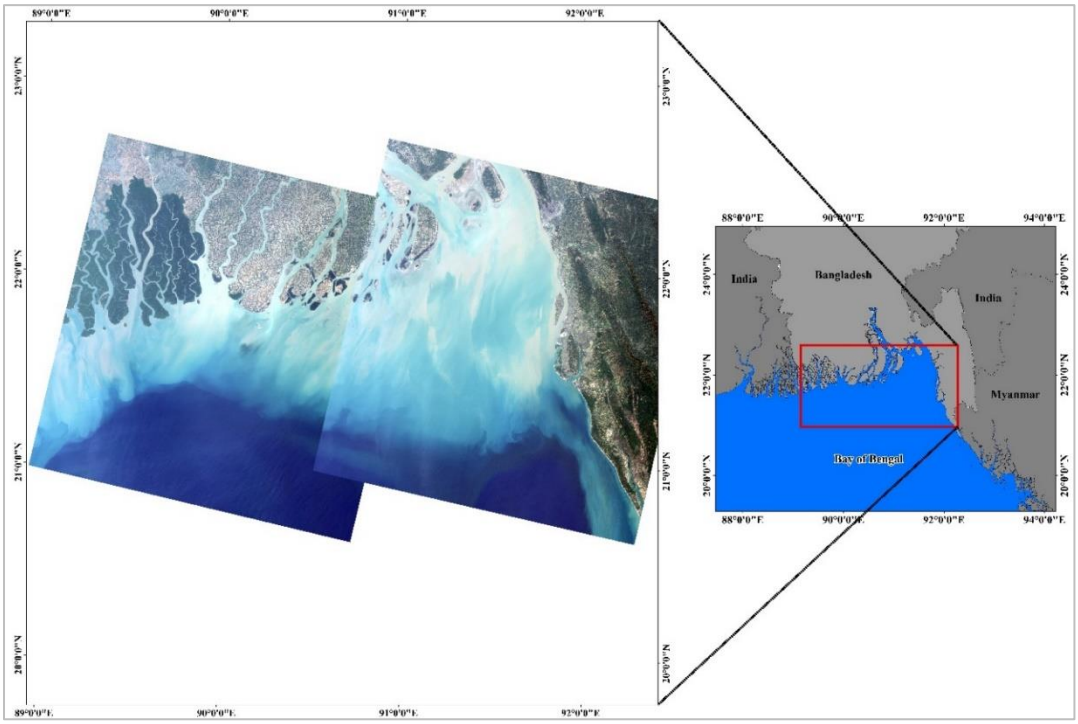

Figure 1: Map showing the study area.

Apart from this, climate change-induced sea-level rise, shoreline sand erosion, and river discharge are driving factors of dynamic changes in the bathymetry of the northern Bay of Bengal. The location was enhanced more distinct by the submarine canyon termed as "Swatch of No Ground," which appears to perforate the bed of the subaqueous river delta and function as a provisional sediment depocenter between the mouth of the river and the submarine Bengal fan (Sarma et al., 2000).

The SW and NE monsoons are the dominant weather cycles in the study area (Hasan et al., 2022). These seasonal variations affect the bathymetry of the BoB by bringing fresh water and sediment from upstream (Fein & Stephens, 1987; Michels et al., 2003). Specifically, the Ganges-

Brahmaputra-Meghna River System contributes about 1 billion tons of sediments annually or 13 million tons daily during the southwest monsoon (Coleman, 1969; Milliman & Syvitski, 1992). As a direct consequence of this, the process that sedimentation has led to the formation of numerous coastal islands, including Bhola, Kutubdia, Moheskhali, Hatiya, Sandwip, Dublar Char, Manpura, Nijhum Dwip, Rangabali, Domar Char, Char Montaz, Sona Char, Char Kukrimukri, Bhasan Char, and others (Curray et al., 1971; Hasan et al., 2021).

The current research area is particularly crucial from a commercial standpoint since it serves as a passageway for marine-based transit and an entryway to the seaports of Bangladesh, namely Chittagong Port, Mongla Port, Matarbari Port, and Payra Port. The area is a hub for several mother vessels, lighter cargo ships, oil tankers, and fishing vessels that carry goods or petroleum to their destinations. Furthermore, the local community's livelihood depends on harvesting various marine fish from the studied coastal area (Hasan et al., 2022).

3. Data and Methods

3.1 Data Collection

In order to pursue the study, three kinds of data were accomplished, including both in-situ and ex-situ data. Hydrographic charts from the Bangladesh NAVY, BIWTA, along with the GEBCO chart, are representations of in-situ data, whilst the remotely sensed imagery was considered ex-situ data. The remotely sensed data were primarily downloaded from the Earth Explorer website of the United States Geological Survey (USGS). For this, two individual Landsat 8 images were extracted (Table 1).

Table 1: Attributes of the two Landsat 8 images.

Portion	WRS Path	WRS Row	Acquisition Date
Western	137	45	December 27, 2020
Central and Eastern	136	45	December 20, 2020

The first image contains mostly the western part of the Bay of Bengal. A band arrangement of red, green, and blue was used in the true-color composite where red is band 4, green is band 3, and blue is band 2. The second image covers mostly the central and eastern parts of the Bay of Bengal. Again, the band combination of red, green, and blue was used to generate the natural color image. The water areas that appeared whitish grey are the shallow water regions near the land, which receive a high level of sediment discharge.

Table 2: Features of the two hydrographic charts.

Charts	Title	Geographic Location	Sounded/ Edition Date	Scale
Bangladesh Navy	Malancha River to St. Martin's Island	Bangladesh	February 05, 2017	1:350000
BIWTA	Hatia, Sandwip & Kumira Channel	Bangladesh	10-18 November & 14-26 December, 2020	1:50000

The two above-mentioned hydrographic charts were used as reference data. The Bangladesh Inland Water Transport Authority (BIWTA) and the Bangladesh Navy Hydrographic and Oceanographic Centre each issued two sets of data (Table 2). They incorporate the multibeam eco-sounding approach, along with some other technologies, to map these data.

Additionally, another bathymetric dataset was derived from the General Bathymetric Chart of the Oceans (GEBCO). As part of the GEBCO Seabed 2030 Project, the Nippon Foundation has collected the most comprehensive and precise global bathymetric data. They employed direct measurement techniques for estimating bathymetry, including single-beam and multi-beam echo-sounding, seismic techniques, and Lidar. Moreover, indirect measurements were carried out using digital bathymetric contours taken from charts, altimetry bathymetry, and electronic navigation charts (GEBCO, 2020).

3.2 Pre-Processing of The Data

Images downloaded for this study had very little cloud coverage, so there was no need to correct the images for cloud-related errors. Landsat 8 has a total of 11 bands, but the ratio transform algorithm only uses a ratio of two. Furthermore, one of the best-performing band pairs is Band 2, the blue band, and Band 3, the green band (Table 3). The spatial resolution of these bands is 30 meters, meaning one pixel represents an area of 30 meters by 30 meters on Earth. Each pixel comes with a DN or Digital Number value that needs to be converted into reflectance values before performing the algorithm. The DN values can be converted into Top of Atmosphere reflectance using the rescaling coefficients of the metadata file that comes with the image. The reference data in raster form were also converted into the vector file format to be used in the analysis.

Table 3: Particulars of the blue and green bands of the Landsat 8 sensor.

Landsat 8 Operational Land Imager (OLI) and Thermal Infrared Sensors (TIRS)			
Bands	Color	Wavelength (micrometers)	Resolution (meters)
2	Blue	0.45 – 0.51	30
3	Green	0.53 – 0.59	30

3.3 Applying Suitable Algorithm

After reviewing some of the algorithms for deriving bathymetry using multispectral satellite imagery, an empirical algorithm called ratio transform was selected for this study that uses a ratio of multiple bands. The Ratio Transform Algorithm was developed by Stumpf et al. (2003) and has been extensively used since then. The general formula is given below:

$$Z = m_1 \cdot \left(\frac{ln(nR_w(\lambda_i))}{ln(nR_w(\lambda_j))} \right) - m_0 \quad (1)$$

Where $R_w(\lambda_i)$ and $R_w(\lambda_j)$ are reflectance values of band i and j, respectively. Here m_1 is a tunable constant that helps to scale the ratio to the actual depth, n is a fixed valued constant for all regions, and m_0 is the offset for the depth of 0 meters.

m_1 and m_0 are usually determined from some reference data or control points. m_0 is nominally the "pseudo-satellite derived bathymetry (SDB)" for the depth of 0 meters. This study used regression lines with a few points from available charts and data to calculate these where m_1 is the slope and m_0 is the intercept of the regression lines. The chart from BIWTA and the GEBCO data were selected as the reference datasets and a few control points were selected from these to determine the values of m_1 & m_0. As per the cluster-based regression, we manually divided each image into several Regions of Interest (ROI) based on their depth. By using the regression method, we developed a few algorithms derived from the equation stated above for both Landsat 8 images. Each algorithm was run using a fundamental tool of the ENVI image processing software.

3.4 Post-Processing

The post-processing step of the study is divided into two segments. One is for showing the correlation between SDB and reference data. And the other one shows the process of generating contour lines via interpolation (Figure 2).

In particular, point shapefiles were generated from Bangladesh NAVY and BIWTA charts. A polygon shapefile was also created from the NAVY chart to mask the land areas from the previously derived output. The point shapefile was used to extract the depths of the GEBCO raster data file. The raster values of the satellite-derived bathymetry were extracted against the reference data (BIWTA and GEBCO) to study the correlation between them. The right column shows the consecutive processes of generating contours from the algorithm results. The raster-to-point conversion tool

was used to convert all the raster values into a point shapefile comprising numerous points. These points were then utilized to interpolate the result using the Inverse Distance Weighted tool. Finally, contour lines were constructed in ArcMap.

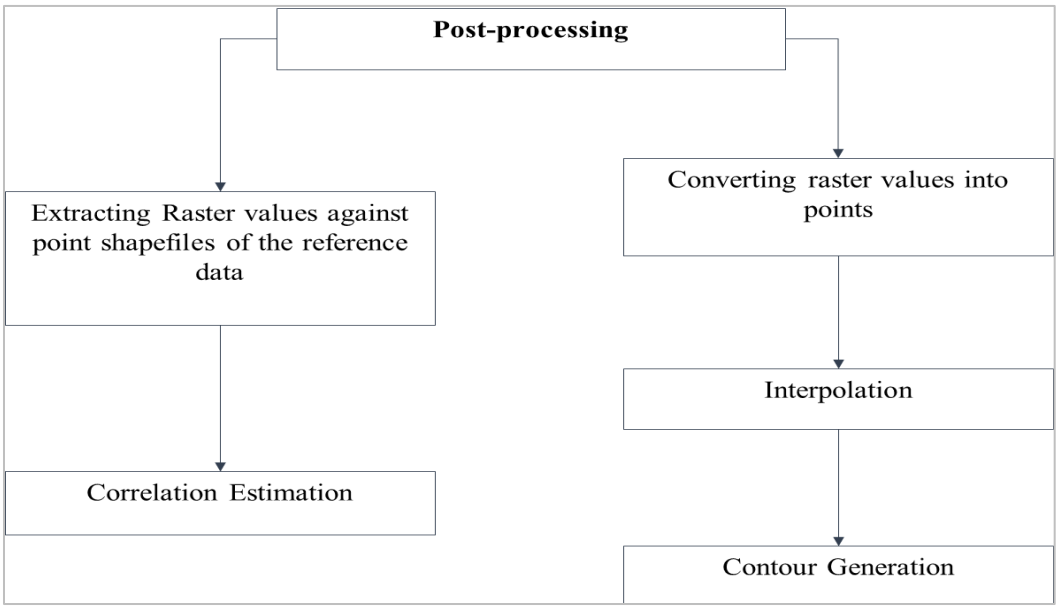

Figure 2: Processes of bathymetry estimation from satellite images.

4. Results and Discussion

Due to the large spatial resolution of Landsat imagery, two images covered the Western, Central, and almost the entire Eastern portion of Bangladesh's coast. After performing the necessary pre-processing strategies, the Ratio Transform Algorithm (RTA) was applied to both images. Since RTA works particularly well in areas with shallow water, this study recorded bathymetry up to a depth of 12 meters. Moreover, for calibration and model validation, the data from Bangladesh NAVY, BIWTA, and GEBCO were extracted up to 12 meters. The respective pixel value from the Satellite-Derived Bathymetry (SDB) was obtained and averaged for each point on the hydrographic charts. Moreover, the same procedure continued to acquire the remaining bathymetry. The statistical index (R^2) is calculated between the satellite-derived value and the reference data to validate the algorithm results.

Figure 3 demonstrates the interpolated result of the Central Coast along with the contour lines, and Figure 4 exhibits R^2 of 0.82 between the satellite-derived bathymetry from the Central Coast and the hydrographic chart of BIWTA. The plotted data shows a root mean square error (RMSE) of 1.06 and a mean absolute deviation (MAD) of 0.89 (Table 4). The reason behind its better performance is that the reference data used to determine the values of m_1 and m_0 were collected from the BIWTA chart, which provides in-situ sounding depths. So, the data from the chart were very reliable, and the timeline of the satellite image and BIWTA chart matched. Also, the chart provided a large number of sounding depths, and the point shapefile created from it contained 5338 soundings. Apart from these, the study utilized the GEBCO gridded data and the Bangladesh NAVY chart as reference datasets for the Western Coast.

Figure 5 illustrates the interpolated result of the Western Coast along with the contour lines, and Figure 6 demonstrates R2 of 0.81 between the satellite-derived bathymetry and the hydrographic chart of Bangladesh NAVY. The plotted data shows an RMSE of 1.55 and a MAD of 1.16 (Table 4). However, even in the turbid waters of the Bay of Bengal, the ratio transform algorithm can extract depths up to 12 meters with very low mean absolute deviations, and root mean squared errors.

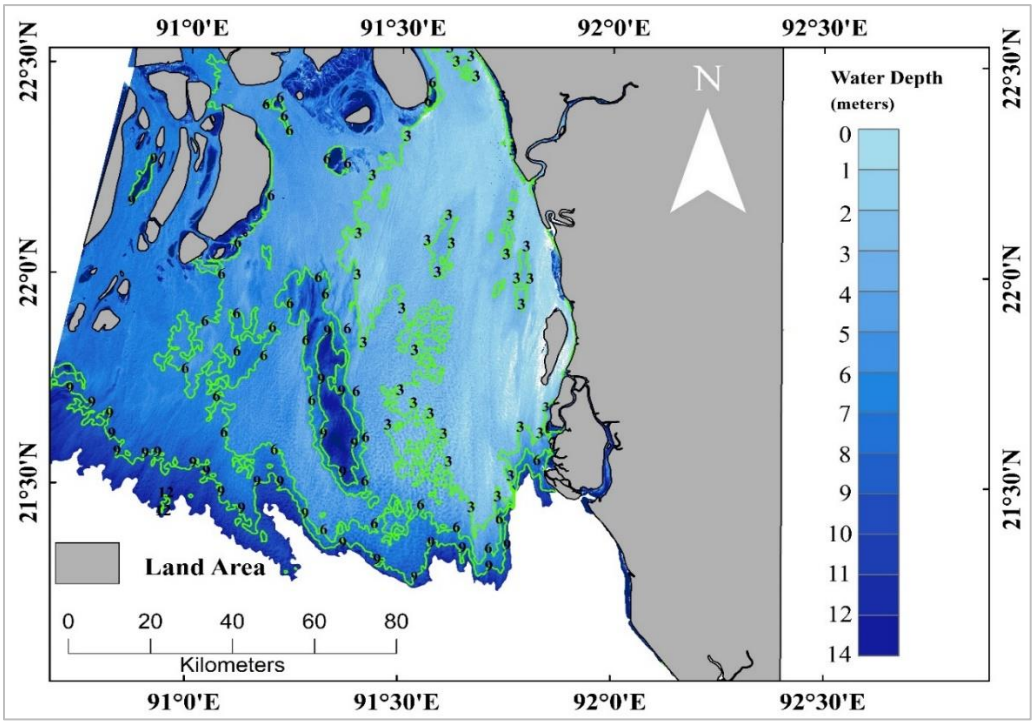

Figure 3: Contours with the interpolated result from the Central and Eastern coast.

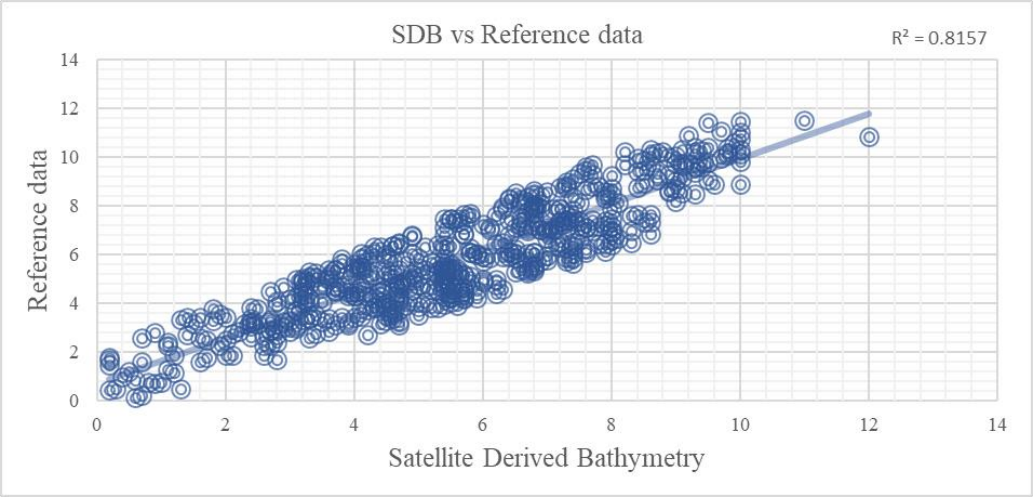

Figure 4: Correlation between the SDB and Reference data for the Central and Eastern coast

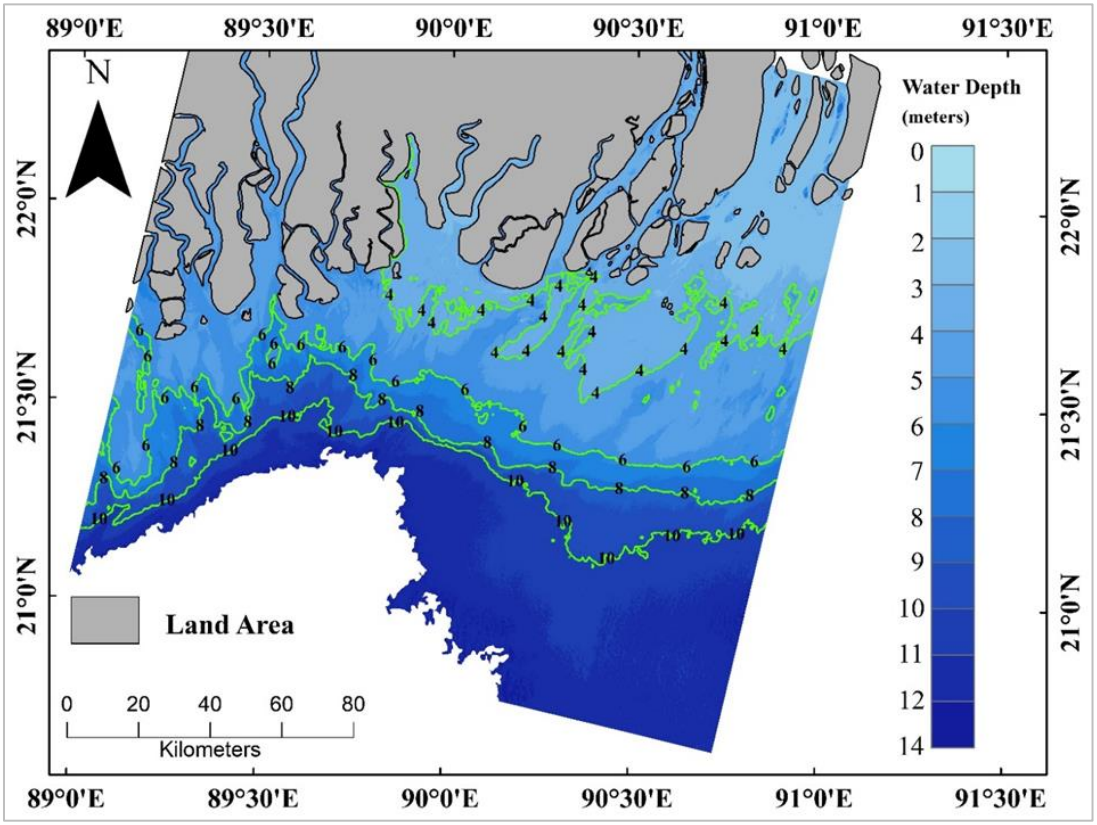

Figure 5: Contours with the interpolated result from the Western coast.

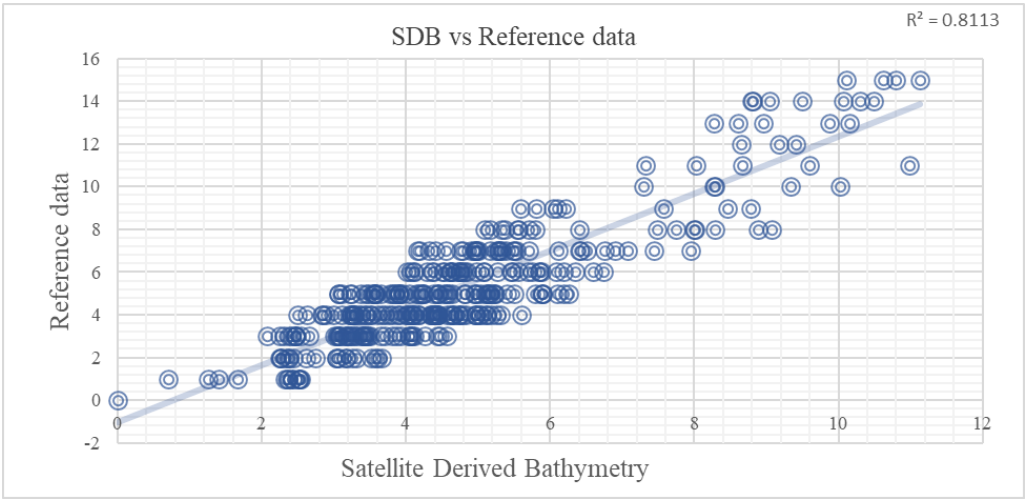

Figure 6: Correlation between the SDB and Reference data for the Western coast.

Table 1: Statistical indices to analyze the accuracy of the model results.

Statistical Indices	R^2 value	MAD	MSE	RMSE
Ratio Transform Algorithm (Central Coast)	0.82	0.89	1.13	1.06
Ratio Transform Algorithm (Western Coast)	0.81	1.16	2.41	1.55

5. Conclusion

The study intended to review and find a suitable method for extracting bathymetry of shallow coastal areas from multispectral satellite imagery. The Ratio Transform Algorithm was tested in this study along the shallow waters of the Bay of Bengal. The algorithm involves the ratio of two bands, and in this case, blue and green bands were used. The algorithm also requires some reference data to determine the slope and intercept of the regression lines. For the reference data, a Bangladesh NAVY hydrographic chart, a BIWTA chart, and GEBCO gridded bathymetry data were collected, and the charts were then digitized.

Two Landsat images were enough to cover almost the whole coastal region of Bangladesh. Hence, the study establishes separate algorithms for the two images and calibrates those using the reference data: the BIWTA chart for the Central Coast and the Bangladesh Navy chart for the Western Coast. After running the algorithms, the R-squared values along with the Mean Absolute Deviation (MAD), Mean Squared Error (MSE), and Root Mean Square Error (RMSE) were calculated for both. Contours were also created after interpolating the results to visualize the study's outcome.

The algorithms performed satisfactorily for Bangladesh's Central, Western, and Eastern coasts up to a depth of 12 meters. Both achieved an R-squared value above 0.8 with Mean Absolute Deviations of 0.89 and 1.16, respectively. Ratio Transform Algorithms tend to produce erroneous results at higher depths since low to moderate-resolution passive sensors cannot penetrate water efficiently due to turbidity. That is why costly active sensors with higher resolution perform better in bathymetry estimation due to their high penetrability in turbid waters.

Acknowledgement

The authors would like to express their gratitude to all those who contributed to this research. The authors are particularly grateful to the Bangladesh Navy Hydrographic Department and the Bangladesh Inland Water Transport Authority (BIWTA) for allowing us to purchase the charts used in this study. Additionally, the authors are grateful to Bangladesh Bank and the Faculty of Earth and Environmental Sciences for providing funds for the study.

References

Adler-Golden, S. M., Acharya, P. K., Berk, A., Matthew, M. W., & Gorodetzky, D. 2005. Remote bathymetry of the littoral zone from AVIRIS, LASH, and QuickBird imagery. IEEE Transactions on Geoscience and Remote Sensing, 43(2), 337–347. https://doi.org/10.1109/TGRS.2004.841246

Ceyhun, Ö., & Yalçın, A. 2010. Remote sensing of water depths in shallow waters via artificial neural networks. Estuarine, Coastal and Shelf Science, 89, 89–96. https://doi.org/10.1016/j.ecss.2010.05.015

Coleman, J. M. 1969. Brahmaputra river: Channel processes and sedimentation. Sedimentary Geology, 3(2–3), 129–239. https://doi.org/10.1016/0037-0738(69)90010-4

Curray, J. R., Moore, D. G., Curray, J. R., & Moore, D. G. 1971. Growth of the Bengal Deep-Sea Fan and Denudation in the Himalayas. GSAB, 82(3), 563. https://doi.org/10.1130/0016-7606(1971)82

Deng, Z., Ji, M., & Zhang, Z. 2008. Mapping Bathymetry from Multi-Source Remote Sensing Images: A Case Study in the Beilun Estuary, Guangxi, China.

Dierssen, H. M., Zimmerman, R. C., Leathers, R. A., Downes, T. V., & Davis, C. O. 2003. Ocean color remote sensing of seagrass and bathymetry in the Bahamas Banks by high-resolution airborne imagery. In Limnol. Oceanogr (Vol. 48, Issue 1).

Doxani, G., Papadopoulou, M., Lafazani, P., Pikridas, C., & Tsakiri-Strati, M. 2012. Shallow-Water Bathymetry Over Variable Bottom Types Using Multispectral WORLDVIEW-2 Image. ISPAr, 39B8, 159–164. https://doi.org/10.5194/ISPRSARCHIVES-XXXIX-B8-159-2012

Duplančić Leder, T., Bačić, S., & Leder, N. 2020. Analysis of State-of-the-Art Hydrographic Survey Technologies Land Surface Temperature View project Satellite Derived Bathymetry View project Nenad Leder Pomorski Fakultet Split Analysis of State-of-the-Art Hydrographic Survey Technologies. https://www.researchgate.net/publication/340809103

Elhassan, I. 2015. Development of Bathymetric Techniques, Kingdom of Saudi Arabia. www.lanfallnavigation.com

Eugenio, F., Marcello, J., & Martin, J. 6357. High-Resolution Maps of Bathymetry and Benthic Habitats in Shallow-Water Environments Using Multispectral Remote Sensing Imagery. IEEE Transactions on Geoscience and Remote Sensing, 53(7), 3539–3549. https://doi.org/10.1109/TGRS.2014.2377300

Fein, J. S., & Stephens, P. L. 1987. Monsoons. 632.

Figueiredo, I. N., Pinto, L., & Gonçalves, G. 2016. A modified Lyzenga's model for multispectral bathymetry using Tikhonov regularization. IEEE Geoscience and Remote Sensing Letters, 13(1), 53–57. https://doi.org/10.1109/LGRS.2015.2496401

GEBCO. 2020. GEBCO Gridded Bathymetry Data. https://www.gebco.net/data_and_products/gridded_bathymetry_data/

Geyman, E. C., & Maloof, A. C. 2019. A Simple Method for Extracting Water Depth From Multispectral Satellite Imagery in Regions of Variable Bottom Type. https://doi.org/10.1029/2018EA000539

Gholamalifard, M., Kutser, T., Esmaili-Sari, A., Abkar, A. A., & Naimi, B. 2013. Remotely Sensed Empirical Modeling of Bathymetry in the Southeastern Caspian Sea. Remote Sensing 2013, Vol. 5, Pages 2746-2762, 5(6), 2746–2762. https://doi.org/10.3390/RS5062746

Hasan, M., Rahman, M., Ahmed, A. al, Islam, M. A., & Rahman, M. 2022. Heavy metal pollution and ecological risk assessment in the surface water from a marine protected area, Swatch of No Ground, north-western part of the Bay of Bengal. Regional Studies in Marine Science, 52, 102278. https://doi.org/10.1016/J.RSMA.2022.102278

Hasan, M., Rahman, M., Islam, M. A., Hossain, M. I. S., Kanak, K., & Azam, O. R. 2021. Assessment of Toxic Heavy Metals in Surface Water of the Meghna River Estuary: An Integrated Statistical Approach. The Dhaka University Journal of Earth and Environmental Sciences, 10(3), 143–155. https://doi.org/10.3329/DUJEES.V10I3.59080

Hell, B., Broman, B., Jakobsson, L., Jakobsson, M., Ke Magnusson, A. °, & Wiberg, P. 2012. The Use of Bathymetric Data in Society and Science: A Review from the Baltic Sea. https://doi.org/10.1007/s13280-011-0192-y

Hogrefe, K. R., Wright, D. J., & Hochberg, E. J. 2008. Derivation and Integration of Shallow-Water Bathymetry: Implications for Coastal Terrain Modeling and Subsequent Analyses. Https://Doi.Org/10.1080/01490410802466710, 31(4), 299–317. https://doi.org/10.1080/01490410802466710

Jagalingam, P., Akshaya, B. J., & Hegde, A. V. 2015. Bathymetry mapping using landsat 8 satellite imagery. Procedia Engineering, 116(1), 560–566. https://doi.org/10.1016/j.proeng.2015.08.326

Kanno, A., Koibuchi, Y., & Isobe, M. 2012. Shallow Water Bathymetry from Multispectral Satellite Images: Extensions of Lyzenga's Method For Improving Accuracy. Https://Doi.Org/10.1142/S0578563411002410, 53(4), 431–450. https://doi.org/10.1142/S0578563411002410

Kerr, J. M., Purkis, S., Kerr, J. M., & Purkis, S. 2018. An algorithm for optically-deriving water depth from multispectral imagery in coral reef landscapes in the absence of ground-truth data. RSEnv, 210, 307–324. https://doi.org/10.1016/J.RSE.2018.03.024

Liang, J., Zhang, J., Ma, Y., & Zhang, C. Y. 2017. Derivation of Bathymetry from High-resolution Optical Satellite Imagery and USV Sounding Data. Http://Dx.Doi.Org/10.1080/01490419.2017.1370044, 40(6), 466–479. https://doi.org/10.1080/01490419.2017.1370044

Liu, S., Gao, Y., Zheng, W., & Li, X. 2015. Performance of two neural network models in bathymetry. Http://Dx.Doi.Org/10.1080/2150704X.2015.1034885, 6(4), 321–330. https://doi.org/10.1080/2150704X.2015.1034885

Lurton, Xavier. 2002. An introduction to underwater acoustics : principles and applications. Springer. https://link.springer.com/book/9783540429678

Lyons, M., Phinn, S., & Roelfsema, C. 2011. Integrating Quickbird Multi-Spectral Satellite and Field Data: Mapping Bathymetry, Seagrass Cover, Seagrass Species and Change in Moreton Bay, Australia in 2004 and 2007. Remote Sensing 2011, Vol. 3, Pages 42-64, 3(1), 42–64. https://doi.org/10.3390/RS3010042

Lyzenga, D. R. 1978. Passive remote sensing techniques for mapping water depth and bottom features. Applied Optics, Vol. 17, Issue 3, Pp. 379-383, 17(3), 379–383. https://doi.org/10.1364/AO.17.000379

Lyzenga, D. R. 1981. Remote sensing of bottom reflectance and water attenuation parameters in shallow water using aircraft and Landsat data. Http://Dx.Doi.Org/10.1080/01431168108948342, 2(1), 71–82. https://doi.org/10.1080/01431168108948342

Lyzenga, D. R., Malinas, N. P., & Tanis, F. J. 2006. Multispectral bathymetry using a simple physically based algorithm. IEEE Transactions on Geoscience and Remote Sensing, 44(8), 2251–2259. https://doi.org/10.1109/TGRS.2006.872909

Ma, S., Tao, Z., Yang, X., Yu, Y., Zhou, X., & Li, Z. 2014. Bathymetry retrieval from hyperspectral remote sensing data in optical-shallow water. IEEE Transactions on Geoscience and Remote Sensing, 52(2), 1205–1212. https://doi.org/10.1109/TGRS.2013.2248372

Ma, Y., Xu, N., Liu, Z., Yang, B., Yang, F., Wang, X. H., & Li, S. 2020. Satellite-derived bathymetry using the ICESat-2 lidar and Sentinel-2 imagery datasets. Remote Sensing of Environment, 250, 112047. https://doi.org/10.1016/J.RSE.2020.112047

Makboul, O., Negm, A., Mesbah, S., & Mohasseb, M. 2017. Performance Assessment of ANN in Estimating Remotely Sensed Extracted Bathymetry. Case Study: Eastern Harbor of Alexandria. Procedia Engineering, 181, 912–919. https://doi.org/10.1016/J.PROENG.2017.02.486

Michels, K. H., Suckow, A., Breitzke, M., Kudrass, H. R., & Kottke, B. 2003. Sediment transport in the shelf canyon "Swatch of No Ground" (Bay of Bengal). Deep Sea Research Part II: Topical Studies in Oceanography, 50(5), 1003–1022. https://doi.org/10.1016/S0967-0645(02)00617-3

Milliman, J. D., & Syvitski, J. P. M. 1992. Geomorphic/Tectonic Control of Sediment Discharge to the Ocean: The Importance of Small Mountainous Rivers. Https://Doi.Org/10.1086/629606, 100(5), 525–544. https://doi.org/10.1086/629606

Misra, A., Vojinovic, Z., Ramakrishnan, B., Luijendijk, A., & Ranasinghe, R. 2018. Shallow water bathymetry mapping using Support Vector Machine (SVM) technique and multispectral imagery. Https://Doi.Org/10.1080/01431161.2017.1421796, 39(13), 4431–4450. https://doi.org/10.1080/01431161.2017.1421796

Pushparaj, J., & Hegde, A. V. 2017. Estimation of bathymetry along the coast of Mangaluru using Landsat-8 imagery. The International Journal of Ocean and Climate Systems, 8(2), 71–83. https://doi.org/10.1177/1759313116679672

Romano, A., & Duranti, P. 2012. Autonomous Unmanned Surface Vessels for Hydrographic Measurement and Environmental Monitoring Autonomous Unmanned Surface Vessels for Hydrographic Measurement and Environmental Monitoring.

Sarma, K. V. L. N. S., Ramana, M. V, Subrahmanyam, V., Krishna, K. S., Ramprasad, T., & Desa, M. 2000. Morphological features in the Bay of Bengal. J. Ind. Geophys. Union, 4(2), 185–190.

Stumpf, R. P., Holderied, K., & Sinclair, M. 2003a. Determination of water depth with high-resolution satellite imagery over variable bottom types. Limnology and Oceanography, 48(1part2), 547–556. https://doi.org/10.4319/LO.2003.48.1_PART_2.0547

Stumpf, R. P., Holderied, K., & Sinclair, M. 2003b. Determination of water depth with high-resolution satellite imagery over variable bottom types. Limnology and Oceanography, 48(1part2), 547–556. https://doi.org/10.4319/LO.2003.48.1_PART_2.0547

Winterbottom, S., & Gilvear, D. 1997. Quantification of channel bed morphology in gravel-bed rivers using airborne multispectral imagery and aerial photography. Regulated Rivers: Research & Management. https://onlinelibrary.wiley.com/doi/abs/10.1002/%28SICI%291099-1646%28199711/12%2913%3A6%3C489%3A%3AAID-RRR471%3E3.0.CO%3B2-X